

ADAPTIVE GRID REFINEMENT IN A BEM-BASED OPTIMAL SHAPE SYNTHESIS

P. HAJELA and J. JIH

Department of Aerospace Engineering, Mechanics and Engineering Science, University of Florida,
Gainesville, FL 32611, U.S.A.

(Received 9 November 1988)

Abstract—The boundary element method is used in conjunction with nonlinear programming methods for optimal structural shape synthesis. An approach for grid refinement and grid adaptation for the boundary element method is developed for application in plane elasticity problems. This technique uses a predefined control function in a variational formulation to obtain an optimal node distribution for the computational domain. To prevent distortion of the original domain, master nodes are introduced to control the geometry of the structure. The paper also describes an efficient implementation of a semi-analytical sensitivity analysis for optimum design. Numerical results are presented for a class of shape synthesis problems.

INTRODUCTION

The determination of an optimal structural shape for desired structural response has been the subject of several recent studies. A general review of papers published during the last decade can be found in Haftka and Grandhi (1986). In most of these efforts (Bennett and Botkin, 1985; Braibant and Fleury, 1985), the finite element method (FEM) is employed as an analytical tool to obtain the structural response. More recently, Choi and Kwak (1988) have focused on the use of the boundary element method (BEM) in the shape design process. The fact that BEM only requires modeling of boundary information renders it a natural candidate for analysis of domain-type problems in optimum shape design (Mota Soares and Choi, 1986).

Kuich (1984) points out several advantages of the boundary element approach over the finite element method in the shape design problem. Among these, the more significant include a replacement of the FEM mesh generation for the entire domain by a boundary discretization in the BEM, a higher accuracy in sensitivity evaluation along the boundary, and simpler preparation of input data for the problem. Furthermore, the level of experience necessary in using BEM is generally not as much as is required in the use of FEM for mesh generation and selection of optimum element sizes. There is, however, some judgement required in obtaining an appropriate discretization of the boundary. Since the geometry of the structural domain changes continuously during the shape design process, an improper grid distribution would yield inaccuracies in stress evaluation, particularly when the geometry is complex. In this paper, a method for automated grid refinement and grid adaptation is introduced to interface with the optimum shape design problem.

In order to obtain more precise analysis results in the boundary element approach, Carey and Kennon (1987) use an approach in which grid points are clustered in regions of large response gradients. For a two-dimensional structural domain, the grid distribution on the boundary is usually treated as an one-dimensional problem. These grid points not only determine the nodes at which analysis is performed, but also define the structural boundary. Hence, proper caution must be exercised so that the structural geometry is not altered when redistributing the nodes for more accurate response analysis. In the present work, this was achieved by the introduction of master nodes, where the latter were not allowed to move during the grid relocation so as to prevent distortion of the original domain.

The concept of grid refinement is similar to the h -method of FEM mesh refinement used by Kikuchi (1986). The structural boundary can be assumed to consist of several zones, with a uniformly spaced grid distribution in each zone. On the basis of a solution

computed from the uniform grid, the grid distribution can be refined locally in each zone. In the proposed approach for grid refinement, a control function is first defined and computed for each zone, and the gradients of this control function determine the number of points that must be removed or added to that zone. After grid refinement, the grid points are redistributed in each zone by an adaptive scheme. A variational approach is chosen in the present work for this adaptive method, as it provides a simple, explicit means of incorporating desired characteristics into the grid generation scheme.

The adaptive mesh generation and refinement approach for the BEM was embedded in an automated optimum design environment. A modified feasible usable search direction algorithm of Vanderplaats (1983) was used for numerical optimization. This approach required the sensitivity of the response quantities with respect to the shape variables, and was obtained by a semi-analytical method. The semi-analytical method is derived from an explicit differentiation of the BEM analysis equations, and takes advantage of the characteristics of these equations. The approach is discussed in a subsequent section of this paper.

BEM IN ELASTICITY PROBLEMS

The boundary element method for elasticity problems derives from Somigliana's identity (Banerjee and Butterfield, 1981), which is given as

$$u_j(\xi) = \int_{\Gamma} [p(x) \cdot G_{ij}(\xi, x) - F_{ij}(\xi, x) \cdot u_j(x)] d\Gamma(x) + \int_{\Omega} b \cdot G_{ij}(\xi, x) d\Omega(x) \quad (1)$$

where u_j is the displacement at point ξ in the j direction; p and b are the actual state of traction and body force, respectively, and $G_{ij}(\xi, x)$ and $F_{ij}(\xi, x)$ represent the Kelvin solutions for displacement and traction at ξ in the j direction due to a unit force applied at x in the i direction. The Kelvin solutions are written as follows,

$$G_{ij}(\xi, x) = \frac{1}{8\pi G(1-\nu)} \left[(3-4\nu) \ln \left(\frac{1}{r} \right) \cdot \delta_{ij} + \frac{\partial r}{\partial x_i} \frac{\partial r}{\partial x_j} \right] \quad (2)$$

$$F_{ij}(\xi, x) = -\frac{1}{4\pi(1-\nu)r} \left[\frac{\partial r}{\partial n} \left\{ (1-2\nu) \cdot \delta_{ij} + 2 \frac{\partial r}{\partial x_i} \cdot \frac{\partial r}{\partial x_j} \right\} - (1-2\nu) \cdot \left(\frac{\partial r}{\partial x_i} \cdot n_j - \frac{\partial r}{\partial x_j} \cdot n_i \right) \right] \quad (3)$$

where

$$r = |x - \xi|.$$

If the field point ξ is close to the boundary, one arrives at an expression involving only the boundary unknowns. Since the singularity point is introduced during the boundary integration, the integral equation (1) assumes the form,

$$C_{ij}u_j(\xi) = \int_{\Gamma} [p(x) \cdot G_{ij}(\xi, x) - F_{ij}(\xi, x) \cdot u_j(x)] d\Gamma(x) + \int_{\Omega} b \cdot G_{ij}(\xi, x) d\Omega(x) \quad (4)$$

where C_{ij} can be expressed as,

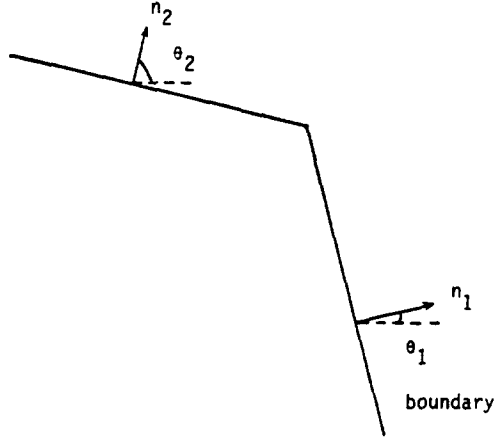


Fig. 1. Definition of domain boundary orientation as defined by angles θ_1 and θ_2 .

$$C_{ij} = \delta_{ij} - I_{ij} \quad (5)$$

where δ_{ij} is the delta function, I_{ij} is defined in terms of θ_1 and θ_2 (Fig. 1), and is written as follows:

$$I_{ij} = -\frac{1}{8\pi(1-\nu)} \begin{bmatrix} 4(1-\nu)(\pi + \theta_2 - \theta_1) & \cos 2\theta_2 - \cos 2\theta_1 \\ + \sin 2\theta_1 - \sin 2\theta_2 & \\ \cos 2\theta_2 - \cos 2\theta_1 & 4(1-\nu)(\pi + \theta_2 - \theta_1) \\ & + \sin 2\theta_2 - \sin 2\theta_1 \end{bmatrix}.$$

C_{ij} is a coefficient that depends on the geometry of the boundary at field point ξ , as in eqn (5), or may be determined from rigid body motion as shown in Brebbia (1978).

The numerical solution of eqn (4) was facilitated by discretizing the boundary into N elements. The values of displacement u and traction p over each element were approximated by using the interpolation function ϕ , expressed in terms of the nodal values u^n and p^n as follows:

$$u = \phi^T u^n \quad (6)$$

$$p = \phi^T p^n. \quad (7)$$

Substitution of expressions for u and p given by eqns (6) and (7) and summing over all the N segments, allows eqn (4) to be expressed in an alternative matrix notation as follows,

$$[H] \cdot \{U\} = [G] \cdot \{P\} + \{B\} \quad (8)$$

where $[H]$ and $[G]$ contain the results of all the integrations. These integrals may be evaluated by any suitable method such as the Gauss quadrature integration scheme. The system of equations (8) can be rearranged in such a way that all unknowns are written on the left-hand side in a vector of unknowns $\{x\}$,

$$[A]\{x\} = \{C\} \quad (9)$$

where $[A]$ is a $N \times N$ matrix and $\{C\}$ is a vector of prescribed boundary values.

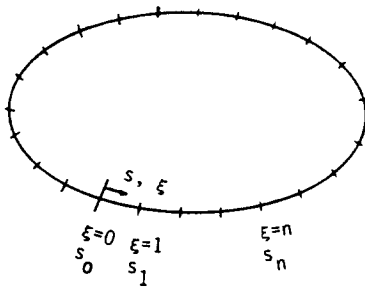


Fig. 2. Definition of boundary and generalized curvilinear coordinates.

ADAPTIVE SCHEME

In the present work, a variational approach was used to obtain an adequate grid for response analysis. The desired features of such a grid were represented in terms of a control function defined along the structural boundary, where larger values of the control function gradients require a proportionately larger number of computational grid points to be assigned to the corresponding region. For a problem pertaining to a one-dimensional adaptation of grid points along the boundary, the boundary coordinates s which defines the length along the boundary, and a generalized curvilinear coordinate ξ which pertains to the computational grid, are shown in Fig. 2. Hindman and Spencer (1983) present one form of a functional I_p , which can be used as a measure of adaptation of the grid spacing in the ξ direction, and is written in terms of a control function P as follows,

$$I_p = \int \frac{\xi_s^2}{P} ds \quad (10)$$

where $\xi_s = \partial\xi/\partial s$, and is referred to as the grid density (number of grid points per unit length). For a one-dimensional problem, the relation between ξ_s and s_ξ is expressed as follows:

$$\xi_s = \frac{1}{s_\xi}. \quad (11)$$

It is observed from eqn (10) that, for the functional I_p to be minimum, a region on the boundary with a small value of control function P would have a corresponding low value of ξ_s . Stated differently, a larger grid spacing is obtained in the region of small P . For a boundary with a fixed number of points, the above implies a denser grid distribution in regions of high P .

The variational approach yields the necessary conditions for optimality that a solution for the grid density must satisfy to extremize the functional I_p . These are the familiar Euler-Lagrange equations, and for the present problem result in a second-order, one-dimensional Poisson equation:

$$\xi_{ss} - \xi_s \cdot P_s/P = 0. \quad (12)$$

This equation governs the location of the grid coordinates in the physical domain. The solution of this equation is facilitated by a transformation to the curvilinear coordinate system. Using a chain rule, the second derivative terms can be shown to be of the following form:

$$\xi_{ss} = -\frac{s_{\xi\xi}}{s_{\xi}^3}. \quad (13)$$

Substituting eqns (11) and (13) into eqn (12) yields the transformed one-dimensional equation for adaptation along the ξ coordinate:

$$s_{\xi\xi} + s_{\xi} \cdot P_{\xi}/P = 0. \quad (14)$$

This equation can be solved directly for the grid point spacing along the ξ -coordinate. Another approach of looking at the adaptation problem is obtained if one integrates eqn (14) once to obtain

$$P \cdot s_{\xi} = C \quad (15)$$

where

$$C = \frac{s_{\Gamma}}{\int \frac{1}{P} d\xi}$$

and s_{Γ} represents the total arc length along the boundary. It is obvious from the above expression that the relationship between the control function P , and the grid point spacing s_{ξ} , is reciprocal.

A proper selection of the control function P is of essence in an adaptive relocation of grid points along the structural boundary. In the problems considered in this exercise, the control function was defined so as to provide adequate clustering of grid points in regions of high stress and high curvature of the boundary. One such control function definition is of the following form,

$$f = \beta \cdot \sigma_v + (1 - \beta) \cdot c_k \quad (16)$$

where f is a control function; σ_v is the Von Mises stress along the boundary; c_k is the curvature of the boundary; β is a weighting factor that assumes values between zero and unity, and determines the relative importance of the stress or curvature in the adaptation process. The ratio of the maximum to the minimum spacing in the computational grid is a measure that should be controllable by a proper selection of a control function. To avoid numerical problems associated with the control function assuming a very small value, a modified control function is defined as follows,

$$P = 1 + \gamma \cdot f \quad (17)$$

where the function f is normalized to range between 0 and 1, and γ is a smoothing factor. The minimum and maximum values of P correspond to $f = 0$ and $f = 1$, respectively. It can be shown that the expression for grid spacing from i to $i+1$ is of the following form,

$$\Delta s_i = \frac{s_{\Gamma} \cdot \frac{1}{1 + \gamma \cdot f_i}}{\sum_j \frac{1}{1 + \gamma \cdot f_j}} \quad (18)$$

where s_{Γ} is the total length of the boundary, and P_i is the value of the control function between i and $i+1$ which can be written as follows:

$$P_i = 1 + \gamma \cdot f_i. \quad (19)$$

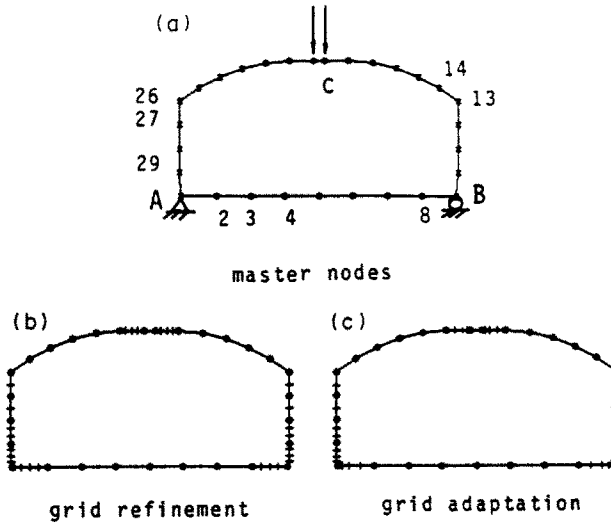


Fig. 3. (a) Structural domain with evenly spaced master nodes. (b) Grid refinement involving the introduction of new evenly spaced grid points in regions of high control function gradients. (c) Grid adaptation based on variational approach.

Hence the ratio of the maximum to the minimum spacing may be expressed as follows :

$$\frac{(\Delta s_i)_{\max}}{(\Delta s_i)_{\min}} = 1 + \gamma. \quad (20)$$

The value of this ratio is clearly dependent on the smoothing factor γ which is prescribed in the control function. However, as explained in subsequent sections, the approach used in this work for grid adaptation and refinement is relatively insensitive to the choice of this parameter.

GRID REFINEMENT AND ADAPTATION

The primary motivation for using an adaptive grid is to allocate an appropriate number of grid points to regions of high stress and curvature. In problems of shape design using the BEM, grid points play a dual role of defining the structural shape and providing discrete points for analysis. In computing the sensitivity of the structural response to changes in the boundary, where the latter is linked to the position of grid points, proper care must be exercised to eliminate distortions in the geometry of the boundary. In the present work, a set of master nodes uniquely define the shape of the structure. These nodes serve as points for response analysis as well as providing the interpolation points for the structural geometry definition. These nodes, shown in Fig. 3(a), are not moved when the adaptive scheme is applied.

Grid adaptation and refinement is essentially a two-stage process. A uniformly distributed grid is first assumed between the master nodes, and the corresponding approximate solution is determined. This solution allows a computation of the control function and its gradient along the boundary. The approach adopted is one in which more grid points are assigned to the high gradient regions, and less or no grid points are located in regions with a smooth variation of the control function. A relatively simplistic scheme was implemented to realize this goal. The numerical values of the gradients of the control function were classified into several levels, and a proportional number of grid points were assigned to each of these levels. The effect of such a redistribution of points based on control function gradients is illustrated in Fig. 3(b).

Once the total number of grid points for each region is determined, the governing equation for grid adaptation is employed to provide a better grid redistribution. This is

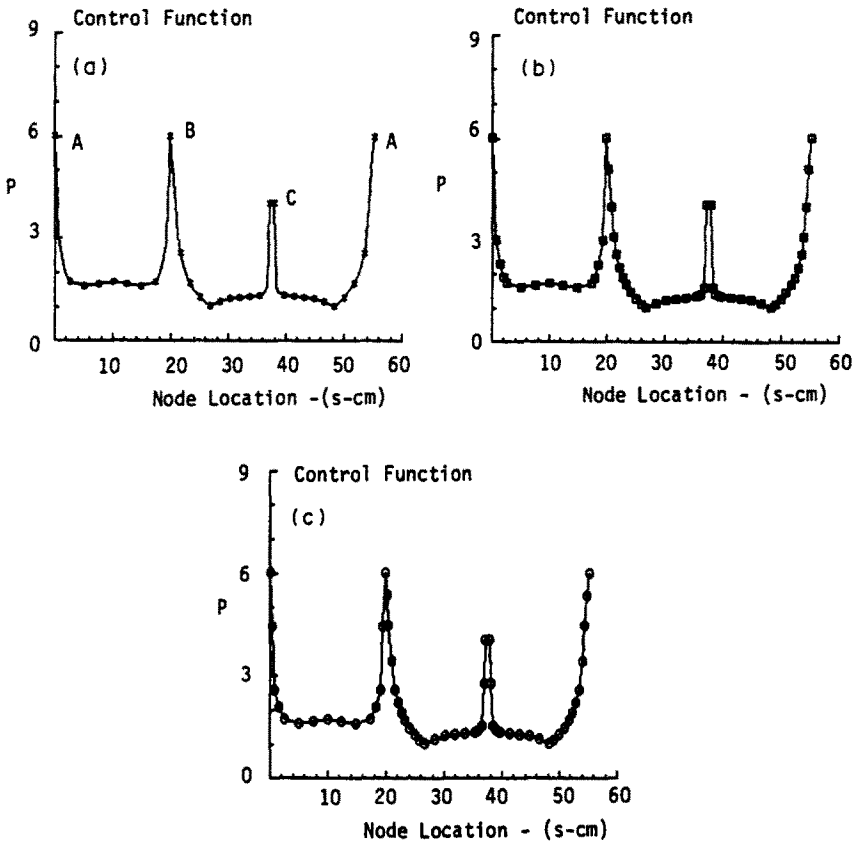


Fig. 4. (a) Control function distribution along the boundary. (b) Grid refinement based on gradients of the control function. (c) Grid adaptation in regions of high stress.

shown in Fig. 3(c). Note that in the solution of eqn (14), the master nodes are always fixed to maintain the boundary of the structure.

Figure 4 illustrates the process of grid point distribution on the basis of control function values. After an approximate solution is obtained for a uniform grid distribution as shown in Fig. 4(a), the grid is refined between each master node on the basis of the gradient of the control function. In Fig. 4(a), we observe that the gradients of the control function around points A, B and C are much higher than elsewhere. Thus, several new grid points are assigned to these regions and evenly distributed within the regions. A smaller number of grid points are assigned to regions of low gradients, as shown in Fig. 4(b). The points placed in these regions are next relocated by a solution of the adaptive equation, and the results of this adaptation are shown in Fig. 4(c). It is worthwhile to bear in mind that since master nodes have been introduced along the boundary, the maximum spacing $(\Delta s_i)_{\max}$ in eqn (20) is equal to the space between each master node. This also renders the adaptation scheme relatively insensitive to the choice of the smoothing factor γ .

Table 1 compares the Von Mises stress distribution along a structural boundary for a problem solved with 149 evenly distributed analytical points, and with 61 analytical points assigned on the basis of grid refinement and adaptation. The differences in the numerical results are small, even though the number of grid points in the second case are less than half the number in the first. Such a reduction of grid points can result in substantial savings in computational cost in shape design problems.

DESIGN SENSITIVITY—SEMI-ANALYTICAL APPROACH

An important ingredient in shape optimization is the computation of sensitivity of the design to the shape variables. The structural shape is governed by a group of independent

Table 1. Comparison of σ_v/σ_{all} for 149 uniformly distributed nodes, and adaptive grid with 61 analytical nodes

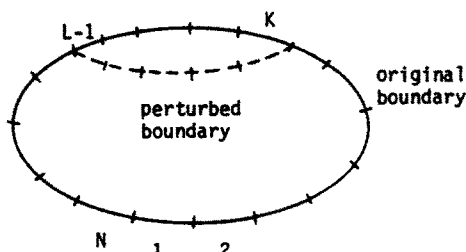
Selected master nodes	$\sigma_v/\sigma_{all}^\dagger$	
	Case 1: uniform grid with 149 analytical nodes	Case 2: adaptive grid with 61 analytical nodes
1	0.8500	0.8629
2	0.1207	0.1197
3	0.0999	0.1029
4	0.1144	0.1121
5	0.1234	0.1185
6	0.1144	0.1121
20	0.5154	0.5092
21	0.0596	0.0595
22	0.0493	0.0538
23	0.0650	0.0480
24	0.0411	0.0404
25	0.0259	0.0254
26	0.0019	0.0096
27	0.0470	0.0484
28	0.1166	0.1144
29	0.2640	0.2690

$^\dagger \sigma_v$ is the Von Mises stress; σ_{all} is the allowable stress (62,000 N cm^{-2}).

design variables, where such variables affect both the objective function (typically weight) and the structural response from which the design constraints are computed. In current applications, the response quantity of interest was the Von Mises equivalent stress in the structure. The sensitivity of this response was computed by a semi-analytical approach, which is an efficient extension of the finite difference method.

A careful examination of the integral eqn (4) indicates that the integral functions H and U , which are functions of $r = |\xi - x|$, are basically determined by the geometry of the structure. When one of the shape design variables is perturbed by a small amount δx , only a portion of the boundary related to that design variable will be changed. It is therefore logical to expect that not all elements in the $[H]$ and $[G]$ matrices are changed during a perturbation of one shape variable. This concept was used in the present work to improve the computational efficiency of the sensitivity analysis.

A better understanding of this idea is obtained by considering the boundary of a structural domain Γ , discretized into several elements as shown in Fig. 5. If one of design variables d_i is disturbed to $d_i + \delta d_i$, the boundary element associated with the design variable d_i will change to Γ' . From the integral eqn (4), one may note that if the load point x is chosen on the unchanged boundary, the difference in matrix elements of $[G]$ and $[H]$, and $[G']$ and $[H']$, where the latter represent the system matrices of the perturbed domain, depends on the location of field point ξ . That is, if the field point ξ is also located on the unchanged boundary, these matrix elements will not be changed. Otherwise, the matrix elements related to the field point ξ which is located on the changed boundary, must be recalculated. Of course, if the load point x lies on the disturbed boundary, the matrix elements related to this load in $[H']$ and $[G']$ will also change.

Fig. 5. Original and perturbed boundaries discretized into N segments.

For simplicity, one may consider a linear interpolation function in eqns (6) and (7). The boundary of structural domain is discretized into N linear segments as shown in Fig. 5. The system equations of the boundary element method can be written as follows:

$$\begin{bmatrix} A_{11} & A_{12} & \dots & A_{1N} \\ A_{21} & A_{22} & \dots & A_{2N} \\ \dots & \dots & \dots & \dots \\ A_{N1} & A_{N2} & \dots & A_{NN} \end{bmatrix} \{x\} = \begin{Bmatrix} C_1 \\ C_2 \\ \vdots \\ C_N \end{Bmatrix}. \quad (21)$$

If one of the design variables, d_i , is perturbed to $d_i + \delta d_i$, boundary elements related to that design variable will be affected. If, for example, the design variable affects boundary elements between those denoted by indices K and $L-1$ (see Fig. 5), new matrices $[A']$ and $\{C'\}$ are obtained as follows,

$$\begin{bmatrix} A'_{11} & A'_{12} & \dots & A'_{1K} & \dots & A'_{1L} & \dots & A'_{1N} \\ A'_{21} & A'_{22} & \dots & A'_{2K} & \dots & A'_{2L} & \dots & A'_{2N} \\ \dots & \dots & \dots & \dots & \dots & \dots & \dots & \dots \\ A'_{K1} & A'_{K2} & \dots & A'_{K2} & \dots & A'_{KL} & \dots & A'_{KN} \\ \dots & \dots & \dots & \dots & \dots & \dots & \dots & \dots \\ A'_{L1} & A'_{L2} & \dots & A'_{LK} & \dots & A'_{LL} & \dots & A'_{LN} \\ \dots & \dots & \dots & \dots & \dots & \dots & \dots & \dots \\ A'_{N1} & A'_{N2} & \dots & A'_{NK} & \dots & A'_{NL} & \dots & A'_{NN} \end{bmatrix} \cdot \{x'\} = \begin{Bmatrix} C'_1 \\ C'_2 \\ \vdots \\ C'_K \\ \vdots \\ C'_L \\ \vdots \\ C'_N \end{Bmatrix} \quad (22)$$

where only those elements within the band are changed.

Differentiating eqn (9) with respect to design variable d_i , the following relation is obtained,

$$[A] \left\{ \frac{\partial x}{\partial d_i} \right\} = \left\{ \frac{\partial C}{\partial d_i} \right\} - \left[\frac{\partial A}{\partial d_i} \right] \{x\} \quad (23)$$

where the matrix $[A]$ on the left-hand side is calculated before the design variable is perturbed. A finite difference approximation is used to obtain the matrix $[\partial A / \partial d_i]$ and the vector $\{\partial C / \partial d_i\}$ as follows,

$$\left[\frac{\partial A}{\partial d} \right] = \frac{[A'] - [A]}{\Delta d_i} \quad (24)$$

$$\left\{ \frac{\partial C}{\partial d} \right\} = \frac{\{C'\} - \{C\}}{\Delta d_i} \quad (25)$$

where $[A']$ and $\{C'\}$ are as obtained in eqn (22), requiring only those elements of $[A]$ and $\{C\}$ to be recalculated that are related to the boundary perturbations.

In the present work, the system equation is first subjected to a LU -decomposition as follows:

$$[A] = [L][U]. \quad (26)$$

The upper and lower triangular matrices, $[U]$ and $[L]$, respectively, are only calculated once and are saved for all subsequent design variable perturbations. After the sensitivities $[\partial A / \partial d_i]$ and $\{\partial C / \partial d_i\}$ are obtained, the solution $\{\partial x / \partial d_i\}$ of eqn (23) is solved in two stages. First,

Table 2. Comparison of operation count for finite difference and semi-analytical approaches to compute design sensitivity.

Finite difference approach	$\frac{N^3}{3}(NDV+1) + N^2(NDV+1) + O(N)$
Semi-analytical approach	$\frac{N^3}{3} + N^2(NDV+1) + O(N)$

$[A]$ is an $N \times N$ matrix; NDV is the number of design variables.

a forward substitution for the lower triangular matrix of $[A]$ results in a solution for $\{H'\}$ as,

$$[L]\{H'\} = \{H\} \quad (27)$$

where

$$\{H\} = \{\partial C/\partial d_i\} - [\partial A/\partial d_i] \cdot \{x\}. \quad (28)$$

This is followed by a backward substitution for the upper triangular matrix of $[A]$:

$$[U]\{\partial x/\partial d_i\} = \{H'\}. \quad (29)$$

In the approach presented above, solution of the system equation for each perturbed design variable to obtain the gradient information is replaced by the backward and forward substitutions. Since the matrix $[A]$ is fully populated, the efficiency of using the semi-analytical approach to the sensitivity analysis is evaluated by an operation count. For a complete set of gradient evaluations, the comparison of operation counts for the finite difference and the semi-analytical approach is shown in Table 2. In comparing with a direct application of the finite difference method, the semi-analytical approach produces computational savings of more than 50%. This is even more significant in the presence of a large number of design variables. Additional savings in computational cost can be realized by selectively computing those elements in the system matrix that are related to perturbations in the boundary.

NUMERICAL RESULTS

The methodology of adaptive grid refinement and calculation of response sensitivity by the semi-analytical method was implemented in the optimum shape sizing of two-dimensional elastic structures. The modified feasible usable search direction algorithm of mathematical programming was combined with a linear boundary element analysis, to obtain an optimization system. The objective of the design is to achieve a minimum volume structure. Constraints included allowable levels of the equivalent Von Mises stress and prescribed lower and upper bounds on the design variables. These design variables were parameters that described the structural geometry. Numerical results for two plane stress problems are presented here.

Example I

A flat plate, supported as shown in Fig. 6, is subjected to a concentrated load of 45,000 N. The allowable stress, Poisson ratio and Young's modulus for the plate material are

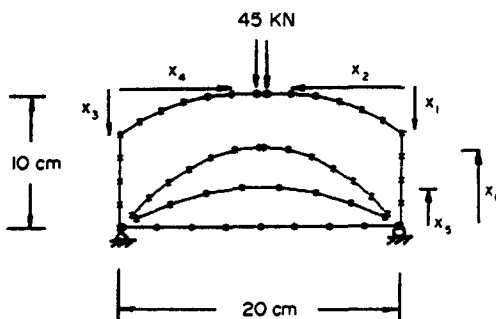


Fig. 6. Definition of geometry and design variables for the elastic plate problem.

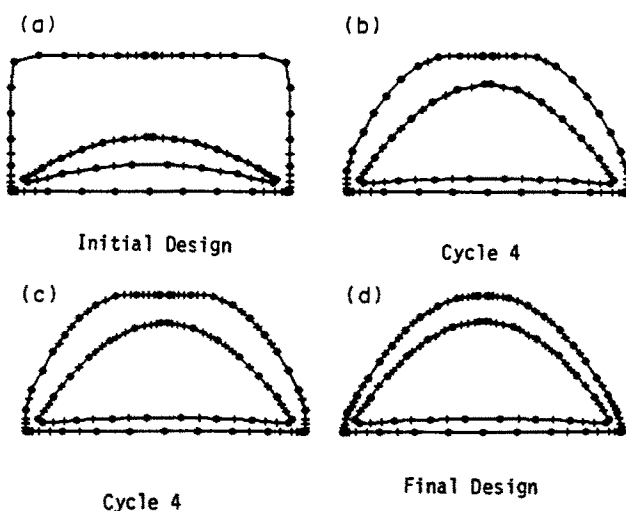


Fig. 7. (a) Initial design for elastic plate problem. (b) Design based on initial grid distribution at beginning of the fourth cycle. (c) New grid distribution at beginning of fourth cycle. (d) Final optimal design for the elastic plate problem.

$62,000 \text{ N cm}^{-2}$, 0.3 , and $2.26 \times 10^7 \text{ N cm}^{-2}$, respectively. The dimensions of the plate and a definition of the shape design variables is also shown in this figure. The distance between the supports is fixed, as are the points A and B. Other boundaries are defined in terms of half-parabolic curves. Design variables x_1 , x_2 and x_3 , x_4 control the right outer and the left outer boundaries, respectively. Design variables x_5 and x_6 define the height of the two parabolic curves on the inner boundary. Symmetry of the loading and support dictates that $x_1 = x_3$ and $x_2 = x_4$.

Figure 7 illustrates the design iteration history for this plate. Starting from the initial design of the structure shown in Fig. 7(a), the design after four cycles is as shown in Fig. 7(b). At this point, the original node distribution is no longer suitable for analysis, and the application of grid refinement and grid adaptation results in a node distribution shown in Fig. 7(c). The optimum shape of the structure is obtained at the sixth cycle, and is shown in Fig. 7(d).

Example II

The second test problem involved the minimum weight design of a fillet to sustain a uniaxial distributed load of $40,000 \text{ N cm}^{-1}$, as indicated in Fig. 8. The material properties are the same as in the previous example. The structural boundary to be redesigned is included between points A and B, as shown in Fig. 8. This boundary was discretized into 10 equal segments, and all nodes on this line (excluding points A and B) were allowed to

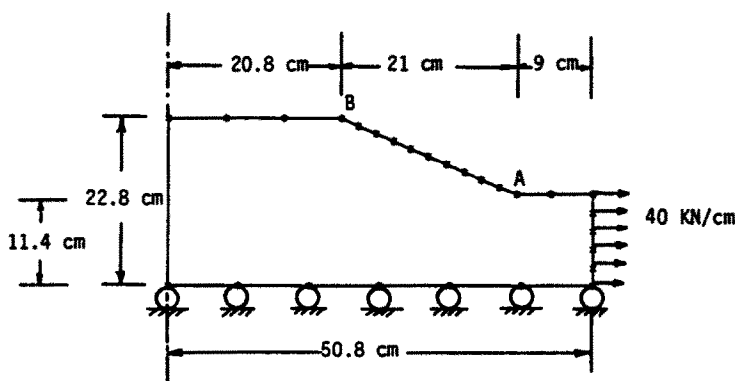


Fig. 8. Definition of geometry and loading for the fillet problem.

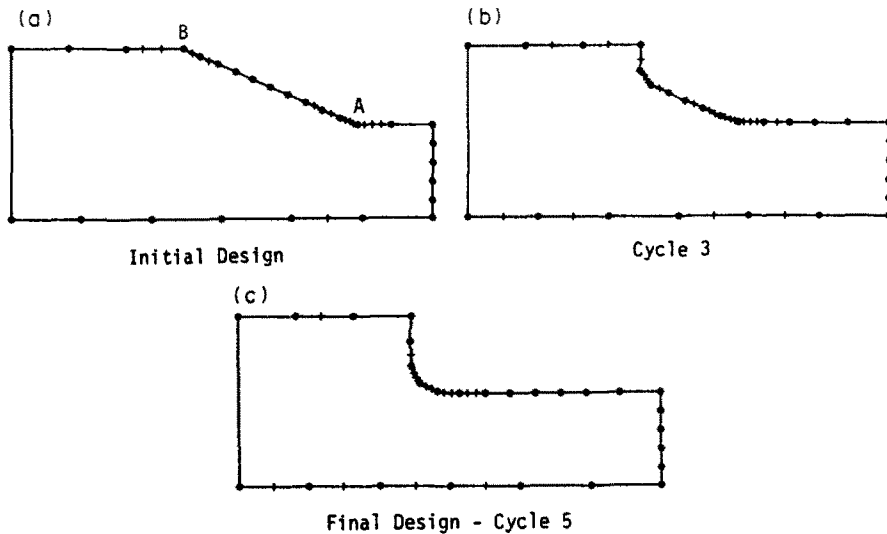


Fig. 9. (a) Initial design for the fillet problem. (b) Design at beginning of third cycle. (c) Final optimal design for the fillet problem obtained at the fifth cycle.

move perpendicular to the line AB during the redesign process. This results in a total of nine design variables for the problem.

This is a classical problem in optimal shape design, and is known to present problems in obtaining a converged optimum. Changes in boundary curvature, particularly the introduction of sharp corners on the boundary, result in significant movements of the zones of high stress. The numerical optimization exploits inherent weaknesses in discrete analysis methods related to the fact that analysis is only performed at predetermined points. The design process, therefore, exhibits an oscillatory behavior. There are essentially two approaches to counter oscillations in such a problem. The first espouses the use of a very large number of points on the boundary to obtain better resolution of regions of high stress. This has the associated drawback of larger computational requirements. The other approach is one which uses grid refinement and adaptation techniques to locate a fewer number of points in the critical regions. The order of the resulting system equations is low, yielding superior computational efficiency.

The initial design for the fillet problem is as shown in Fig. 9(a). An adaptive grid was defined and the design allowed to proceed with prescribed move limits on each design variable during the optimization. The presence of such move limits alleviates the computational burden to some extent, as a new grid refinement is not necessary after each iteration. Figures 9(b) and 9(c) illustrate the progression of the design to an optimum.

CLOSING REMARKS

The present paper discusses some key ideas related to an efficient optimal shape synthesis of elastic structures. The boundary element method is used for analysis as it provides better accuracy in response computations at the boundary. A gradient-based, nonlinear programming algorithm is employed for optimization. The evaluation of such gradients is done by semi-analytical methods, where such methods are shown to be significantly more efficient than difference approximations. This concept of gradient evaluation can be readily extended to other classes of problems. The paper also describes an effective approach for grid refinement and adaptation in shape synthesis problems. In using such an adaptive scheme, the order of system equations in the BEM analysis can be reduced significantly.

Acknowledgement—Computational support received under a grant from the Pittsburgh Supercomputer Center is gratefully acknowledged.

REFERENCES

- Banerjee, P. K. and Butterfield, R. (1981) *Boundary Element Method in Engineering Science*. McGraw-Hill, London.
- Bennett, J. A., and Botkin, M. E. (1985). Structural shape optimization with geometric description and adaptive mesh refinement. *AIAA JI* **23**, 458–464.
- Braibant, V. and Fleury, C. (1985). An approximation-concept approach to shape optimal design. *Comp. Meth. Appl. Mech. Engng* **53**, 119–148.
- Brebbia, C. A. (1978). *The Boundary Element Method for Engineering*. John Wiley, New York.
- Carey, G. F. and Kennon, S. (1987). Adaptive mesh redistribution for a boundary element (panel) method. *Int. J. Num. Meth. Engng* **24**, 2315–2325.
- Choi, J. H. and Kwak, B. M. (1988). Boundary integral equation method for shape optimization of elastic structures. *Int. J. Num. Meth. Engng* **26**, 1579–1595.
- Haftka, R. T. and Grandhi, R. V. (1986) Structural shape optimization—A survey. *Comp. Meth. Appl. Mech. Engng* **57**, 96–106.
- Hindman, R. G. and Spencer, J. (1983). A new approach to truly adaptive grid generation. AIAA paper 83-0450. AIAA 21st Aerospace Sciences Meeting, Reno, January 1983.
- Kikuchi, N. (1986). Adaptive grid-design method for finite element analysis. *Comp. Meth. Appl. Mech. Engng* **55**, 129–160.
- Kuich, G. (1984). Starting to work with boundary element technique in computer aided engineering. In *Boundary Element Techniques in Computer-aided Engineering* (Edited by C. A. Brebbia). Martinus Nijhoff, Dordrecht.
- Mota Soares, C. A. and Choi, K. K. (1986). Boundary element technique in shape optimal design of structures. In *The Optimum Shape* (Edited by J. A. Bennett and M. E. Botkin). Plenum Press, New York.
- Vanderplaats, G. N. (1983). A robust feasible directions algorithm for design synthesis. *Proc. 24th AIAA ASME/ASCE/AHS Structures, Structural Dynamics, and Materials Conf.*, Lake Tahoe, Nevada, 2–4 May 1983.